Article

Mechanoprotection by Polycystins against Apoptosis Is Mediated through the Opening of Stretch-Activated K$_{2P}$ Channels

Rémi Peyronnet,[1] Reza Sharif-Naeini,[1] Joost H.A. Folgering,[1] Malika Arhatte,[1] Martine Jodar,[1] Charbel El Boustany,[1] Claire Gallian,[1] Michel Tauc,[2] Christophe Duranton,[2] Isabelle Rubera,[2] Florian Lesage,[1] York Pei,[3] Dorien J.M. Peters,[4] Stefan Somlo,[5] Frederick Sachs,[6] Amanda Patel,[1] Eric Honoré,[1,7,*] and Fabrice Duprat[1,7]

[1]Institut de Pharmacologie Moléculaire et Cellulaire, UMR CNRS 7275, Université de Nice Sophia Antipolis, 06560 Valbonne, France
[2]CNRS-FRE 3427, Transport Ionique, Aspects Normaux et Pathologiques Université de Nice-Sophia Antipolis, 06108 Nice Cedex 2, France
[3]Divisions of Nephrology and Genomic Medicine, University Health Network and University of Toronto, Toronto, Ontario M5G 2N2, Canada
[4]Department of Human Genetics, Leiden University Medical Center, P.O. Box 9600, 2300 RC Leiden, The Netherlands
[5]Department of Internal Medicine, Yale University School of Medicine, New Haven, CT 06520-8056, USA
[6]Centre for Single Molecule Biophysics, SUNY at Buffalo, Buffalo, NY 14214, USA
[7]These authors contributed equally to this work
*Correspondence: honore@ipmc.cnrs.fr
DOI 10.1016/j.celrep.2012.01.006

SUMMARY

How renal epithelial cells respond to increased pressure and the link with kidney disease states remain poorly understood. *Pkd1* knockout or expression of a PC2 pathogenic mutant, mimicking the autosomal dominant polycystic kidney disease, dramatically enhances mechanical stress-induced tubular apoptotic cell death. We show the presence of a stretch-activated K$^+$ channel dependent on the TREK-2 K$_{2P}$ subunit in proximal convoluted tubule epithelial cells. Our findings further demonstrate that polycystins protect renal epithelial cells against apoptosis in response to mechanical stress, and this function is mediated through the opening of stretch-activated K$_{2P}$ channels. Thus, to our knowledge, we establish for the first time, both in vitro and in vivo, a functional relationship between mechanotransduction and mechanoprotection. We propose that this mechanism is at play in other important pathologies associated with apoptosis and in which pressure or flow stimulation is altered, including heart failure or atherosclerosis.

INTRODUCTION

Mechanical forces play a central role in early development, as well as in various important physiological functions, including hearing, touch, or the regulation of heart rate (Chalfie, 2009; Garcia-Anoveros and Corey, 1997; Lumpkin and Caterina, 2007; Pedersen and Nilius, 2007; Wozniak and Chen, 2009). Various organs have the ability to adapt and cope with high mechanical forces. For instance, resistance arteries reduce their diameter in response to hypertension so that, according to the law of Laplace, they maintain their wall tension constant (Mulvany, 2002).

Failure to adapt to high mechanical forces (flow or pressure) results in cell death and contributes to pathological states, including atherosclerosis and cardiac hypertrophy (Hahn and Schwartz, 2009; Jaalouk and Lammerding, 2009). How cells sense mechanical forces and how they adapt to mechanical stress are not yet fully understood.

Stretch-activated ion channels (SACs) show an increase in open probability (Po) in response to pressure (Kung, 2005; Sachs and Morris, 1998). The TREK-1, TREK-2, and TRAAK two-pore potassium channel (K$_{2P}$) subunits underlie the stretch-activated K$^+$-selective channels (SAKs) (for review, see Honoré, 2007). TREK-1, the most thoroughly studied SAK, is thought to be directly activated by tension in the lipid bilayer (Honoré et al., 2006; Patel et al., 1998). Moreover, channel opening can also be reversibly induced, in the absence of mechanical stimulation, by a variety of anionic amphipathic molecules, including the long-chain polyunsaturated fatty acid docosahexaenoic acid (DOHA), as well as by intracellular acidosis (Honoré, 2007). TREK-2 shares all the functional properties of TREK-1, besides its sensitivity to external pH (Bang et al., 2000; Lesage et al., 2000; Sandoz et al., 2009). Transcellular Na$^+$/glucose or Na$^+$/amino acid cotransports in amphibian renal proximal convoluted tubules (PCTs) have been associated with water influx and an increase in cellular volume resulting in the opening of basolateral SAKs sharing the functional properties of the cloned TREK/TRAAK K$_{2P}$ channels (Beck and Potts, 1990; Cemerikic and Sackin, 1993; Sackin, 1989).

Autosomal dominant polycystic kidney disease (ADPKD) is caused by mutations in either *PKD1* (85% of the patients) or *PKD2* (15% of the patients) genes, encoding the polycystins PC1 and PC2 (Delmas, 2004; Harris and Torres, 2009; Patel and Honoré, 2010; Wilson, 2004; Zhou, 2009). PC1 includes a prominent extracellular amino-terminal domain, 12 transmembrane segments, and a short intracellular carboxy-terminal domain. PC2 is a member of the TRP family of calcium channels containing a pore sequence between transmembrane segments 5 and 6. Both proteins interact through their cytosolic
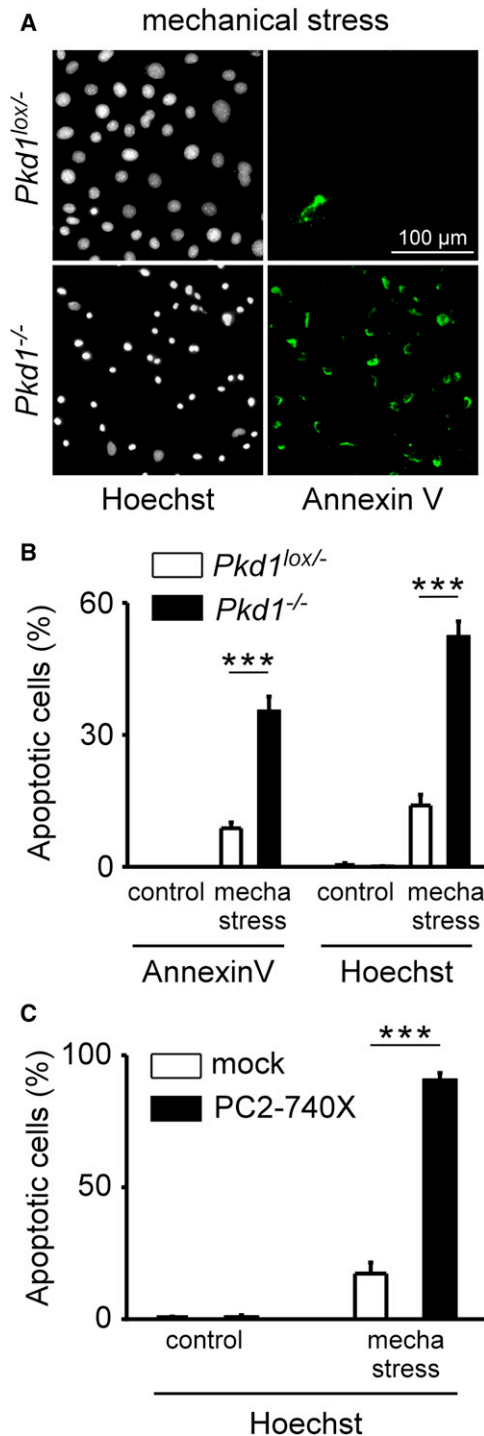
A

mechanical stress

Pkd1^{lox/-}

Pkd1^{-/-}

100 µm

Hoechst   Annexin V

B

□ *Pkd1^{lox/-}*
■ *Pkd1^{-/-}*

Apoptotic cells (%)

***   ***

control mecha stress   control mecha stress

AnnexinV   Hoechst

C

□ mock
■ PC2-740X

Apoptotic cells (%)

***

control   mecha stress

Hoechst

Figure 1. Polycystins and Mechanical Stress-Induced PCT Cell Death

(A) Early apoptosis detected by annexin V labeling (visualized in green as shown on the right panels) induced by mechanical stress (4 hr at ~2,800 × *g*) in both *Pkd1^{lox/−}* (top) and *Pkd1^{−/−}* (bottom) culture-plated PCT cells. Total number of nuclei and late-cell death is detected by a Hoechst staining (shown in black and white on the left panels).

(B) Histogram showing the amount of early (annexin V) and late (Hoechst) apoptosis induced by mechanical (mecha) stress in both *Pkd1^{lox/−}* (n = 18

carboxy-terminal coiled-coil domains. The polycystin complex has been previously shown to act as a flow sensor in the primary cilium of both renal epithelial and endothelial cells (Nauli et al., 2003, 2008). Moreover, polycystin dosage was recently demonstrated to regulate arterial pressure sensing (Sharif-Naeini et al., 2009). In arterial myocytes we have shown that polycystins regulate the activity of the SACs responsible for the myogenic tone, but the molecular identity of these channels was not defined (Sharif-Naeini et al., 2009).

Although less than 1% of the tubules become cystic in ADPKD, a gradual decrease in glomerular filtration rate (GFR) ultimately leads to kidney failure (Grantham et al., 2011). Why so few cysts impair the function of so many nephrons (about 1 million) in the kidney is still an open question. Although cystogenesis results from an increase in cell proliferation, apoptosis of both cystic and noncystic tubular cells is also documented in ADPKD (Boca et al., 2006; Boletta et al., 2000; Edelstein, 2005; Goilav, 2011; Tao et al., 2005; Woo, 1995). In an experimental model of ADPKD, up to 50% of the glomeruli become atubular, with loss of the glomerulotubular junction cells (Tanner et al., 2002). Compression/obstruction of noncystic "healthy" tubules by growing cysts and/or fibrosis was proposed to result in an upstream tubular dilation (Grantham et al., 2011; Power et al., 2004). Moreover, abnormal fluid accumulation causes the cyst wall to stretch (Derezic and Cecuk, 1982). Thus, an increase in intrarenal mechanical stress leading to apoptosis is also proposed to be associated with kidney failure in ADPKD (Grantham et al., 2011).

In the present report we demonstrate that polycystins play a key role in protecting renal epithelial cells against apoptosis in response to mechanical stress, and this function is mediated through the opening of stretch-activated K_{2P} channels.

RESULTS

Mechanical Stress-Induced PCT Cell Death Is Influenced by Polycystins

In order to study the effect of mechanical stress on cultured PCT cells, we developed an in vitro assay based on centrifugal force. Mouse PCT cells plated on glass coverslips were spun for 4 hr at 2,800 × *g*, and after a recovery period of 3 hr, early apoptosis was quantified by detecting the externalization of phosphatidylserine (annexin V assay) and a later event of cell death by visualizing DNA condensation (Hoechst staining) (Figure 1A). To examine the role of PC1, we used an immortalized mouse PCT *Pkd1^{−/−}* cell line derived from a parental *Pkd1^{lox/−}* clone following transfection with Cre recombinase (Wei et al.,

plates with 19,000 cells analyzed) and *Pkd1^{−/−}* PCT cells (n = 18 plates with 36,000 cells analyzed).

(C) Histogram showing the amount of late apoptosis (Hoechst staining) induced by mechanical stress in both mock (n = 12 plates with 1,300 transfected cells analyzed) and PC2-740X (n = 11 plates with 250 transfected cells analyzed) transiently transfected cultured PCT cells. Transfected cells were visualized by EGFP fluorescence (green), and nuclear fragmentation was evaluated by Hoechst staining. Cell death was determined 3 hr after mechanical stress.
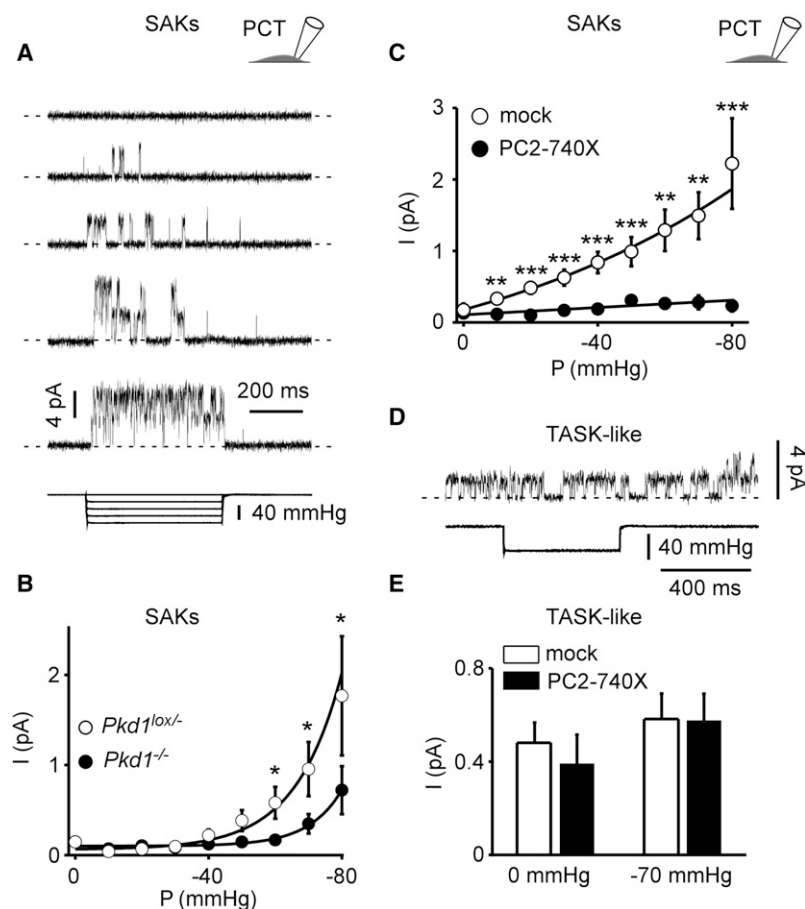
Data represent mean ± SEM. ***p < 0.001.

Figure 2. Polycystins Regulate SAK Activity in PCT Cells

(A) SACs were recorded in the cell-attached patch configuration at a holding potential of 0mV in immortalized mouse PCT cells. The pipette solution contained 5 mM K$^+$, and the reversal potential of these channels was estimated to be about −80mV (see Figure S1). Channel activity is illustrated at increasing negative pressure applied at the back of the patch pipette. Pressure pulses are shown at the bottom. Two channels were active in this patch. The zero current is indicated by a dashed line.

(B) Pressure-effect curves for mean pressure-induced currents recorded in the cell-attached patch configuration in $Pkd1^{lox/−}$ (empty circles; n = 142) and in $Pkd1^{−/−}$ (filled circles; n = 146) PCT cells. Same conditions as in (A).

(C) Mean SAK currents in PCT cells transiently transfected with either a mock empty pIRES$_2$-DsRed plasmid (empty circles; n = 97) or together with PC2-740X (filled circles; n = 82). Currents were recorded in the cell-attached patch configuration at a holding potential of 0mV.

(D) TASK-like channel activity recorded in the same conditions as in (A). These channels are not responsive to an increase in pressure as shown in the lower trace.

(E) The histogram shows the effect of PC2-740X (n = 31), as compared to the mock empty expression vector (n = 33) on TASK-like channel activity in PCT cells.

Data represent mean ± SEM. *p < 0.05; **p < 0.01; ***p < 0.001.

about −80mV, indicating K$^+$ selectivity (see Figure S1 available online). SAKs were recorded in tubular epithelial cells either maintained in primary culture or following immortalization (Figure 2A, and see later Figure S3C). Channel openings gradually and reversibly increased with applied negative pressure and eventually reached saturation (Figure 2A).

Interestingly, SAK activity was significantly reduced in the $Pkd1^{−/−}$ cells, as compared to the heterozygote parental $Pkd1^{lox/−}$ cells (Figure 2B). Next, we studied the effect of the pathogenic mutant PC2-740X transiently expressed in WT PCT cells (Figure 2C). PC2-740X expression similarly induced a dramatic inhibition of SAK activity at all pressures studied (Figure 2C). The single-channel current amplitude (i) of SAKs measured at 0mV was not altered by PC2-740X (4.1 ± 0.1 pA, n = 35 and 4.1 ± 0.1 pA, n = 14 for mock and PC2-740X, respectively), indicating that either the number of active channels (n) or the Po is decreased by PC2-740X (as I = n × Po × i; with I being the mean current). PCT cells also express a constitutively active K$^+$ channel resistant to TEA, 4AP, and glibenclamide and which is not modulated by membrane stretch (Figures 2D and 2E). This channel has previously been documented to be responsible for volume regulation of PCT cells and shown to be encoded by the alkaline-activated K$_{2P}$ channel subunit TASK-2 (Barriere et al., 2003; L'Hoste et al., 2007). Importantly, the native TASK-like channels in PCT cells were not affected by expression of PC2-740X, although SAKs were inhibited in the same cells (Figures 2C–2E). These findings indicate that polycystins specifically modulate native SAK activity in PCT cells.
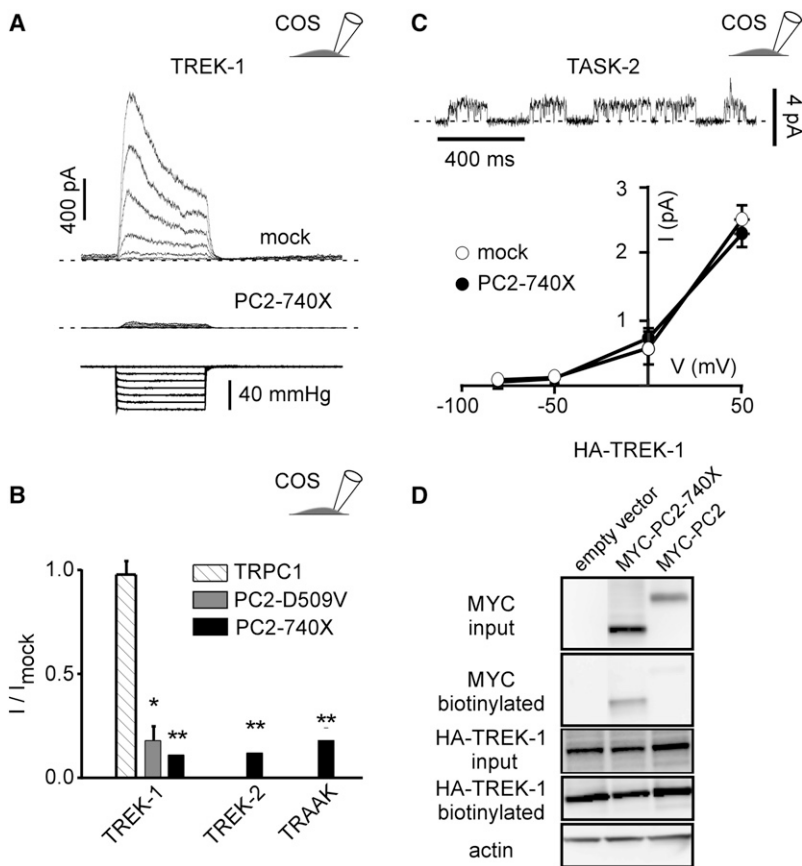
2008) (Figures 1A and 1B). Homozygote inactivation of $Pkd1$ significantly increased PCT cell death induced by mechanical stress, which was absent in the control condition (Figures 1A and 1B). In subsequent experiments we studied the effect of the pathogenic mutant PC2-740X expressed in wild-type (WT) mouse PCT cells (Figure 1C). Similarly, PC2-740X expression dramatically increased the level of PCT cell death induced by mechanical stress (Figure 1C). These findings indicate that polycystins greatly influence the sensitivity of PCT cells to mechanical stress and associated cell death.

The Stretch Sensitivity of SAKs/K$_{2P}$ Channels Is Conditioned by Polycystins

We next examined whether SACs might be involved in the response of renal cells to mechanical stimulation. Using the cell-attached patch-clamp configuration coupled to a fast-pressure clamp system, we identified SAKs in mouse PCT epithelial cells (Figure 2A). These channels were recorded at a holding potential of 0mV in the presence of TEA (10 mM), 4-aminopyridine (3 mM), and glibenclamide (10 μM) in the pipette medium in order to minimize possible contamination by BK, K$_V$, or K$_{ATP}$ channels. The single-channel conductance of SAKs recorded in the presence of 5 mM extracellular K$^+$ was 49.7 ± 0.2 pS (n = 5), and a reversal potential was extrapolated to be

Figure 3. Stretch Activation of TREK/TRAAK K$_{2P}$ Channels Expressed in COS Cells Is Inhibited by PC2-740X

(A) TREK-1 currents (top trace) recorded in the cell-attached patch configuration at a holding potential of 0mV in transiently transfected COS cells (cotransfected with a mock empty pIRES$_2$-DsRed plasmid) in response to increasing negative pipette pressure from 0 to −60 mm Hg in steps of −10 mm Hg (bottom trace). When coexpressed with PC2-740X, the amplitude of the stretch-activated current is dramatically reduced (middle trace).

(B) Mean current ratios (I/I$_{mock}$) for TREK-1, TREK-2, or TRAAK at a holding potential of 0mV in COS cells co-transfected with empty expression vector (n = 112), TRPC1 (n = 20), PC2-740X (n = 27, 27, and 22), or PC2-D509V (n = 28) in the cell-attached patch configuration at a pressure of −60 mm Hg.

(C) TASK-2 currents in a transfected COS cell (together with a mock empty pIRES$_2$-DsRed plasmid) recorded in the cell-attached patch configuration at a holding potential of 0mV. I-V curves for TASK-2 in the absence (together with the empty expression vector; n = 9) or in the presence of PC2-740X (n = 6).

(D) Biotinylation experiments of TREK-1 in transfected COS cells. Neither PC2-740X nor WT PC2 affects expression of TREK-1 at the plasma membrane in COS cells. The three conditions tested are HA-TREK-1 plus empty vector, HA-TREK-1 plus MYC-PC2-740X, and HA-TREK-1 plus MYC-PC2. Input blot and biotinylation blot were either probed with anti-MYC to detect PC2 or anti-HA to detect TREK-1. Blots were then stripped and probed with anti-actin. Only the input blot showed an actin signal that was equivalent for all three lanes. No detectable difference in TREK-1 expression at the cell surface was seen between any of these conditions.

Data represent mean ± SEM. *p < 0.05; **p < 0.01.

Because SAKs in PCT cells share the functional properties of the cloned TREK/TRAAK K$_{2P}$ channels (Honoré, 2007), we investigated whether these recombinant channels might similarly be regulated by polycystins. The TREK-1, TREK-2, and TRAAK K$_{2P}$ channel subunits were expressed transiently in COS cells, and stretch-induced activity was recorded in the cell-attached patch configuration as previously described (Figures 3A and 3B). No endogenous SAKs were present in this mock-transfected cell line (Patel et al., 1998). Coexpression with the mutant PC2-740X significantly reduced the stretch-induced TREK-1, TREK-2, or TRAAK currents (Figures 3A and 3B). Stretch activation of TREK-1 was also significantly impaired by PC2-D509V coexpression, another pathogenic mutant reported to exert a dominant-negative effect (Bai et al., 2008; Ma et al., 2005; Sammels et al., 2010) (Figure 3B). In contrast, TREK-1 channel activity was not altered by coexpression with TRPC1, a PC2-interacting TRP subunit (Tsiokas et al., 1999) (Figure 3B). Notably, PC2-740X failed to affect exogenous TASK-2 channels coexpressed in COS cells (Figure 3C).

A possible mechanism for TREK/TRAAK inhibition by PC2 mutation may involve an effect on the biosynthesis and/or trafficking of the TREK/TRAAK channels. However, biotinylation experiments performed in transiently transfected COS cells demonstrate that the plasma membrane expression of the TREK-1 subunits is not altered by overexpression of PC2-740X, suggesting that instead channel gating might be altered (Figure 3D). Biotinylation experiments also confirm that WT PC2 is mostly retained in the endoplasmic reticulum, whereas the PC2-740X mutant is targeted to the plasma membrane (Chen et al., 2001) (Figure 3D). These results indicate that stretch sensitivity of the cloned TREK/TRAAK K$_{2P}$ channels is impaired by expression of PC2 pathogenic mutants.

Are the General Gating Properties of SAKs Modulated by Polycystins?

Because TREK/TRAAK channels are polymodal, activated by both physical and chemical stimuli, we next investigated whether the general gating properties of SAKs/TREK/TRAAK channels might be affected by PC2-740X. Besides activation by membrane stretch, native SAKs are also opened by intracellular acidosis, either induced by addition of 90 mM extracellular HCO$_3^-$ in the cell-attached patch configuration or directly by lowering intracellular pH in the inside out configuration (Maingret et al., 1999) (Figures 4A, S2A, and S2B). Remarkably, the activation by HCO$_3^-$ was not affected by PC2-740X (Figures 4A and 4B). However, in the same patches and in the absence of HCO$_3^-$, pressure activation of native SAKs in PCT cells was strongly inhibited by PC2-740X (Figure 4B). In TREK-1 transfected COS cells, PC2-740X expression similarly failed to affect HCO$_3^-$ current stimulation in the cell-attached patch
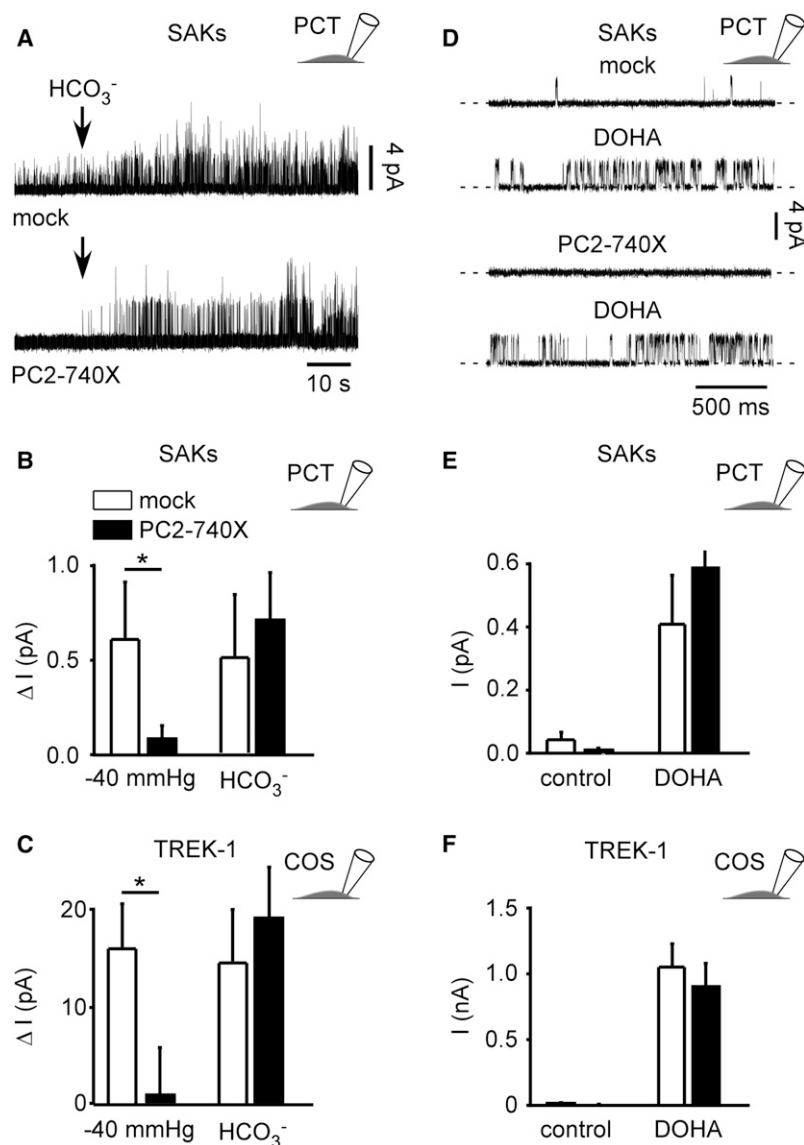
Figure 4. Stimulation of SAK/TREK-1 Activity by Intracellular Acidosis or DOHA Is Not Altered by PC2-740X

(A) Addition of 90 mM HCO_3^- in the bath solution induced SAK activity in the cell-attached patch configuration at a holding potential of 0mV in mock-transfected PCT cells (top) or in PC2-740X transfected PCT cells (bottom).

(B) Changes in mean SAK current amplitude in mock (empty bars; n = 5) or PC2-740X (filled bars; n = 5) expressing PCT cells induced in the same patches by stretch (−40 mm Hg) or HCO_3^- addition (0 mm Hg).

(C) Changes in TREK-1 mean current amplitude in mock (empty bars; n = 28) or PC2-740X (filled bars; n = 21) co-expressing COS cells induced by HCO_3^- addition (0 mm Hg) or stretch (−40 mm Hg).

(D) Cell-attached patch recording of SAKs in a mock-transfected PCT cell at a holding potential of 0mV in control condition (0 mm Hg) including 0.01% ethanol (vehicle; top trace) or after extracellular addition of 10 μM DOHA (second trace). Same with expression of PC2-740X (bottom two traces).

(E) Changes in mean SAK current amplitude (0 mm Hg) in the absence or in the presence of DOHA (10 μM) in PCT cells transfected either with a mock empty plasmid (empty bars; n = 8) or together with PC2-740X (black bars; n = 8).

(F) Changes in mean TREK-1 current amplitude (0 mm Hg) in the absence or in the presence of DOHA (10 μM) in coexpressing COS cells transfected either with a mock empty plasmid (empty bars; n = 12) or together with PC2-740X (black bars; n = 13).

Data represent mean ± SEM. *p < 0.05.

configuration (Figure 4C). Intracellular acidosis has been previously shown to protonate the residue E306 in the cytosolic carboxy-terminal domain of TREK-1, resulting in constitutive channel opening (Honoré et al., 2002). Substitution of E306 by an alanine mimics protonation and locks the channel in the open conformation. The E306A mutant expressed in COS cells, which shows a background activity resistant to membrane stretch, was again not altered by coexpression with PC2-740X (Figure S2C).

Native SAKs in PCT cells, as well as TREK-1 expressed in transfected COS cells, were also reversibly stimulated by external addition of the long-chain polyunsaturated fatty acid DOHA (Figures 4D–4F). Again, the DOHA-induced activity was not significantly altered by expression of PC2-740X (Figures 4D–4F).

These results show that although the stretch sensitivity of the SAKs/TREK/TRAAK channels is strongly inhibited by PC2-740X, activation by intracellular acidosis or polyunsaturated fatty acids is resistant. Thus, these findings indicate that polycystins specifically regulate SAK/TREK/TRAAK mechanogating.

Inhibition of SAK Mechanogating by PC2-740X Involves the Actin Cytoskeletal Network

Our previous findings have established that TREK-1 channel activity induced by stretch is repressed by F-actin (Lauritzen et al., 2005). We explor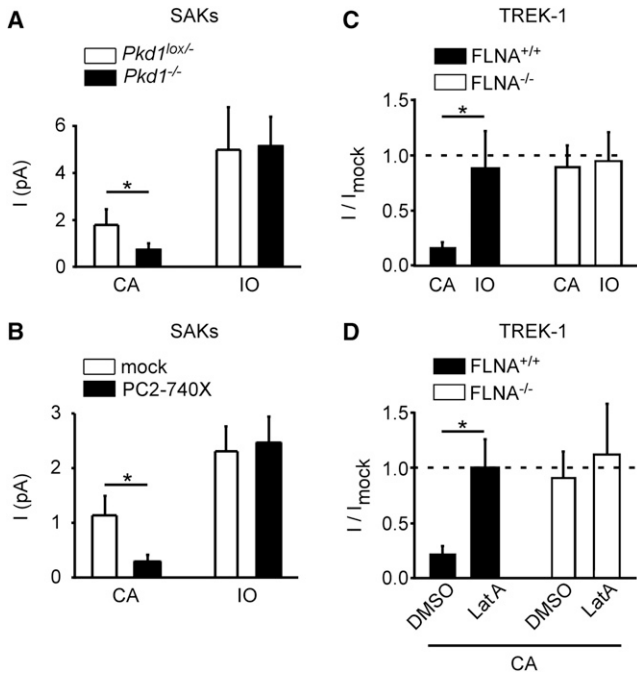ed the possibility that polycystins may affect pressure-dependent TREK/TRAAK channel activity through the F-actin cytoskeleton network.

The actin cytoskeleton can be mechanically disrupted by excision of the patches in the inside out configuration (Lauritzen et al., 2005). When *Pkd1* is inactivated or when PC2-740X is expressed in PCT cells, SAK inhibition, which is observed in the cell-attached patch configuration, disappeared upon excision of the patches in the inside out configuration (Figures 5A and 5B). Similarly, when transfected in FLNA$^{+/+}$ cells (A7 cells), which express the PC2 interactor filamin A, an actin-crosslinking protein, again TREK-1 inhibition is reversed by patch excision (Figure 5C). By contrast in the FLNA$^{-/-}$ cells (M2 cells), inhibition was absent in both cell-attached and inside out patch configurations (Figure 5C). Rescue of channel activity upon patch excision suggests that the cytoskeleton is involved in the downregulation of SAKs/TREK/TRAAK by polycystins. Indeed,

Figure 5. Role of the Actin Cytoskeleton in the Regulation of SAK/TREK-1 Mechanogating by Polycystins

(A) SAK activity elicited by membrane stretch (−80 mm Hg) in the cell-attached (CA) patch configuration is significantly reduced in the $Pkd1^{-/-}$ (n = 20), as compared to the $Pkd1^{lox/-}$ PCT cells (n = 21). SAK activity induced by stretch in the $Pkd1^{-/-}$ cells is rescued following patch excision in the inside out (IO) patch configuration.

(B) SAK activity elicited by membrane stretch (−60 mm Hg) in the cell-attached patch configuration is significantly reduced by PC2-740X expression (black bars; n = 12), as compared to mock-transfected PCT cells (white bars; n = 15). SAK activity induced by stretch in the PC2-740X expressing cells is rescued following patch excision in the inside out patch configuration.

(C) SAK activity in A7 cells (FLNA$^{+/+}$) is strongly reduced by PC2-740X expression (black bars; n = 21), as compared to the mock condition (n = 21). Patch excision in the inside out configuration rescues channel activity (black bar; n = 17). When transfected in M2 cells (FLNA$^{-/-}$), PC2-740X fails to affect TREK-1 channel activity elicited by stretch in both the cell-attached (white bar; n = 44) and the inside out (white bar; n = 15) patch configurations. Pressure stimulation was −60 mm Hg. The dashed line indicates I/Imock = 1.

(D) Latrunculin A treatment (3 μM) reverses TREK-1 inhibition by PC2-740X expression in FLNA$^{+/+}$ cells in the cell-attached patch configuration (black bars; n = 33), as compared to mock condition (n = 17). In FLNA$^{-/-}$ cells, no inhibition by PC2-740X is seen, and latrunculin A fails to affect channel activity (white bars; n = 21 and n = 13). Pressure stimulation was −60 mm Hg. The dashed line indicates I/Imock = 1.

Data represent mean ± SEM. *p < 0.05.

treating FLNA$^{+/+}$ cells with latrunculin A, which disrupts the F-actin cytoskeleton, also reversed TREK-1 inhibition in the cell-attached patch configuration, although it failed to affect channel activity in the FLNA$^{-/-}$ cells lacking filamin A (Figure 5D). These findings indicate that F-actin and filamin A are critically required for the regulation of SAK/TREK/TRAAK mechanogating by polycystins.

SAK Knockout Enhances Tubular Cell Death Induced by Mechanical Stress

Native SAKs recorded in PCT cells share the functional properties of both TREK-1 and TREK-2 subunits, which are similarly activated by stretch, DOHA, and intracellular acidosis, unlike TRAAK, which is activated by intracellular alkalosis. In the subsequent experiments we aimed to identify which TREK subunit encodes for the native SAKs in PCT cells. The TREK-2 subunit has previously been shown to be expressed in the kidney (Bang et al., 2000; Lesage et al., 2000). Indeed, we detected expression of TREK-2 in whole tubules and in cultured immortalized PCT cells by qPCR (Figures S3A and S3B). Although TRAAK was also found in whole tubules (including distal tubules), it was very low in PCT cells (Figures S3A and S3B). SAK activity was lost in TREK-2$^{-/-}$ PCT cells either maintained in primary culture or after immortalization, recorded both in the cell-attached and excised inside out patch configurations (Figure S3C). The TASK-like channel activity was, however, still present in the TREK-2$^{-/-}$ cells (Figure S3D).

We examined the renal structure of constitutive TREK-2 knockout (KO) adult mice maintained in basal conditions. These kidneys were not different from those of control WT mice (Figure S4). Furthermore, in the $Pkd1^{+/-}$ background, TREK-2 homozygote KO did not show any obvious structural defect (Figure S4). To avoid any possible confounding genetic compensation mechanisms and to be able to inactivate the three stretch-activated K$_{2P}$ channels at the same time, in subsequent experiments we used a mouse model in which the genes encoding TREK-1, TREK-2, and TRAAK have been knocked out altogether (SAK KO) (Guyon et al., 2009). Again, no kidney structural defect was visible in adult SAK KO mice (Figure S4).

We next hypothesized that a loss of SAK activation may influence PCT cell death induced by mechanical stress. We compared the sensitivity to centrifugal force (as described earlier) of WT PCT cells with those of SAK KO PCT cells in which the stretch-activated TREK/TRAAK K$_{2P}$ channels have been deleted altogether. SAK KO PCT cells were consistently more sensitive to mechanical stress-induced cell death, as compared to WT PCT cells (Figures 6A and 6B).

We reasoned that a loss of SAK stretch sensitivity may influence tubular cell death in a high intrarenal pressure condition. We used a mouse model of ureteral obstruction that is associated with increased intrarenal pressure and wall stress (Power et al., 2004; Quinlan et al., 2008; Rohatgi and Flores, 2010; Wyker et al., 1981). We performed unilateral ureteral ligation for 3 days in 10-day-old mice (Figures 6C–6G). The dimension of the obstructed kidneys after 3 days of obstruction significantly increased to a similar extent in both WT and SAK KO mice (Figures 6C and S5). A close-up view of the kidney structure demonstrates that tubules were significantly dilated upon ureteral obstruction, irrespective of the genotype (Figures 6D and 6E). Obstructive uropathy is associated with apoptosis of epithelial cells and tubular atrophy (Power et al., 2004; Quinlan et al., 2008; Rohatgi and Flores, 2010). We measured apoptosis by a double Hoechst and TUNEL staining in the obstructed, in the unligated contralateral, as well as in the sham-operated kidneys from both WT and SAK KO mice. No apoptosis was detected in sham-operated kidneys (n = 9; data not shown) or in the
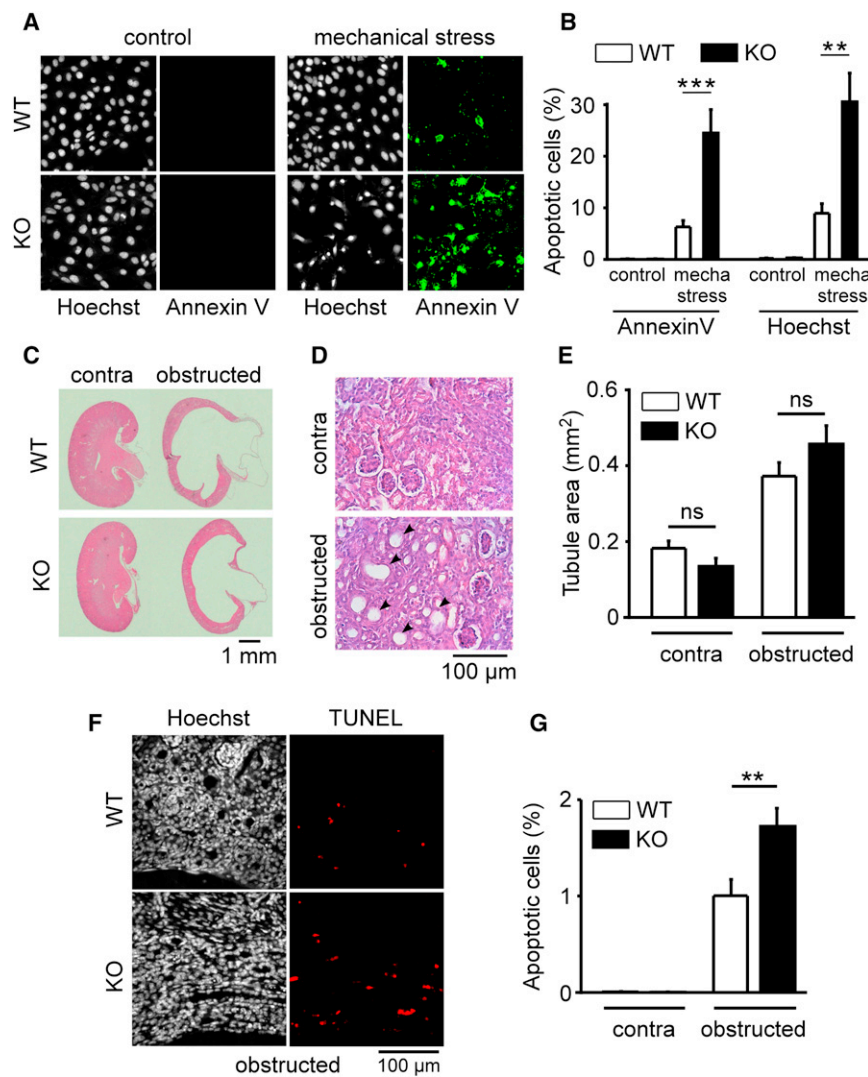
Figure 6. SAK KO Increases Mechanical Stress-Induced PCT Cell Death Both In Vitro and In Vivo

(A) Early apoptosis visualized by annexin V labeling (panels in green on the right) induced by mechanical stress (centrifugal force) in both WT (top) and SAK KO (TREK-1$^{-/-}$/TREK-2$^{-/-}$/TRAAK$^{-/-}$) (bottom) cultured PCT cells. Total number of nuclei and late apoptosis is detected by a Hoechst staining (panels in black and white on the left).

(B) Histogram showing the amount of early (annexin V) and late (Hoechst) apoptosis induced by mechanical (mecha) stress in both WT (n = 11) and SAK KO PCT cells (n = 12). Cell death was determined 3 hr after mechanical stress (centrifugation of plated cells at 2,800 × g for 4 hr).

(C) Sections of WT and SAK KO (TREK-1$^{-/-}$/TREK-2$^{-/-}$/TRAAK$^{-/-}$) mouse contralateral (contra; left panel) or obstructed (right panel) kidneys stained with hematoxylin and eosin.

(D) Effect of ureteral ligation on the tubular diameter of a WT kidney from a 10-day-old mouse ligated for 3 days (bottom), as compared to the contralateral (contra) kidney (top). Kidney sections were stained with hematoxylin and eosin.

(E) Tubular area cross section of contralateral (contra) and obstructed kidneys from WT (white bars; n = 7) and SAK KO (black bars; n = 6) mice. ns, nonsignificant.

(F) Ureteral ligation increases the number of apoptotic cells as detected by a double Hoechst (left panels) and TUNEL staining (right panels in red).

(G) Effect of ureteral ligation on apoptotic cell death (TUNEL staining) in kidneys from WT (white bars; n = 14) and SAK KO (black bars; n = 13) mice. contra, contralateral.

Data represent mean ± SEM. **p < 0.01; ***p < 0.001.

contralateral kidneys (Figures 6G and S6). By contrast about 1% of the tubular cells were found apoptotic in the WT obstructed kidneys, in agreement with previous reports (Power et al., 2004; Quinlan et al., 2008; Rohatgi and Flores, 2010; Wyker et al., 1981) (Figures 6F and 6G). Remarkably, the number of apoptotic cells almost doubled in the obstructed kidneys from SAK KO mice lacking the stretch-activated K$_{2P}$ channels (Figure 6G). These findings demonstrate that TREK/TRAAK K$_{2P}$ channels are protective against tubular epithelial cell death induced by mechanical stress both in vitro and in vivo.

DISCUSSION

The present study shows that when SAKs are inactivated, similarly to *Pkd1* KO or PC2 pathogenic mutant expression mimicking ADPKD, PCT cells in vitro become highly sensitive to mechanical stress and undergo apoptosis. Moreover, our in vivo findings further indicate that the opening of the TREK/TRAAK channels is protective against apoptosis associated with high intrarenal pressure. We identify, and demonstrate at the molecular level, the regulation of SAKs (K$_{2P}$ channels) by polycystins in the kidney. Altogether, these findings show that mechanoprotection by polycystins against apoptosis is mediated through the opening of stretch-activated K$_{2P}$ channels. These molecular findings are significant to better understand how polycystins regulate pressure sensing in the kidney.

Is the regulation of SAKs by polycystins specific? Native or exogenous TASK-2 channels (another K$_{2P}$ channel) are not altered by PC2-740X expression, whereas in the same PCT cells, SAKs are inhibited. PC2-740X also fails to affect other types of ion channels such as voltage-gated K$^+$ channels or ASICS (Sharif-Naeini et al., 2009). In addition, PC2-740X does not influence the E306A TREK-1 gain-of-function mutant. SAK inhibition is not seen with TRPC1, another TRP channel subunit. Importantly, we provide evidence using biotinylation experiments, that the plasma membrane expression of TREK-1 is not altered by PC2-740X. Remarkably, when we excise patches in the inside out configuration, SAK activity is fully rescued, demonstrating

that channels are still present at the plasma membrane, but their stretch sensitivity is specifically repressed by PC2-740X expression in the cell-attached configuration. Moreover, low pH_i or DOHA activation of SAKs in the cell-attached configuration is not altered, again demonstrating that channels are functional at the plasma membrane when PC2-740X is expressed, although their stretch activation is strongly repressed. These findings indicate that the pathogenic mutant PC2-740X selectively inhibits the stretch sensitivity of K_{2P} channels. Our previous study demonstrated that polycystins also regulate the stretch sensitivity of nonselective SACs in arterial myocytes (Sharif-Naeini et al., 2009). Because the loss-of-function PC2 D509V mutant similarly inhibits SAK mechanogating, PC2 permeation is unlikely to be involved in this effect.

Potassium channel activity has been shown to be proapoptotic in both neuronal and non-neuronal cells (for review, see Patel and Lazdunski, 2004). For instance the TASK-2 K_{2P} channels play a key role in PCT cell apoptotic volume decrease (AVD) (L'Hoste et al., 2007). By contrast in the present study we demonstrate a protective role for SAKs (i.e., TREK/TRAAK K_{2P} channels) against mechanical stress-induced cell death. Failure to repolarize could be an important factor in the initiation of stretch-induced cell death (Kainulainen et al., 2002). Opening of SAKs in PCT cells during mechanical stimulation is anticipated to protect cells from excessive depolarization. Another possible explanation for mechanoprotection by SAKs might be related to cell swelling associated with Na^+/solute cotransport, previously shown to be coupled to SAK activity at the basolateral membrane of PCT cells (Beck and Potts, 1990; Cemerikic and Sackin, 1993; Sackin, 1989). Although the present findings suggest that stretch activation of SAKs during mechanical stress protects PCT cells from apoptosis, constitutive TREK/TRAAK channel activity is anticipated to have an opposite effect. Indeed, our previous work indicates that constitutive (or leak) K_{2P} channel activity such as TREK-1 E306A is proapoptotic, unlike WT TREK-1 (Lauritzen et al., 2003). These results indicate that SAK mechanogating is probably central to its protective effect. Cells will hyperpolarize during mechanical stress because of the opening of SAKs. Is the hyperpolarization, or the change in intracellular K^+ resulting from the K^+ efflux, or both, linked with cellular mechanoprotection? We have performed in vitro mechanical stimulation of PCT cells for 4 hr (centrifugal force) and subsequently measured intracellular K^+ concentration. No significant difference is seen between control and SAK KO cells before or after mechanical stress (data not shown). Thus, it is unlikely that K^+ itself is involved in the protective effect of SAKs. We propose that cell hyperpolarization is a key parameter in mechanoprotection by SAKs.

Urinary tract obstruction, which is the leading cause of pediatric end-stage renal failure, notably provokes tubular cell apoptosis (Chevalier, 2008). In line with this clinical observation, previous experimental findings indicate that there is a close association between tubular distension and apoptosis in the kidney (Grantham et al., 2011; Power et al., 2004; Quinlan et al., 2008; Wyker et al., 1981). In the present study, inactivation of SAK K_{2P} channel subunits significantly enhances tubular cell apoptosis in an experimental model of ureteral obstruction in the newborn mouse. These results show that opening of SAKs

exerts a protective effect on tubular epithelial cells subjected to chronic stretch. It would be interesting to stimulate SAK opening during ADPKD, with an expected protection of renal cells. Unfortunately, to our knowledge, because neither a specific opener nor a SAK gain-of-function mouse model is yet available, this experiment cannot be performed at the present time.

Thus, resistance to apoptosis induced by high intrarenal pressure involves mechanotransduction (i.e., opening of mechano-gated potassium channels). To our knowledge, this is the first time that a functional link is established between mechanotransduction and mechanoprotection. TREK and TRAAK channels are broadly expressed, including in cardiac and arterial myocytes, as well as in endothelial cells (Blondeau et al., 2007; Garry et al., 2007; Terrenoire et al., 2001). Thus, our findings may be extended to other pathologies associated with apoptosis and in which pressure or flow stimulation is altered, including cardiac hypertrophy/heart failure or atherosclerosis (Hahn and Schwartz, 2009; Jaalouk and Lammerding, 2009).

Here, we demonstrate that upon *Pkd1* inactivation or expression of a PC2 pathogenic mutant, mimicking ADPKD, inhibition of the stretch sensitivity of SAKs is deleterious and contributes to increased tubular apoptosis. In ADPKD a "two hit" mechanism was put forward to explain focal cystogenesis, slow progression of the disease, and the interfamily phenotypic variability (Qian et al., 1996; Wu et al., 1998). However, several observations also suggest that an additional dosage mechanism may be at play in the disease (Lantinga-van Leeuwen et al., 2004; Pei, 2001). If polycystin dosage is indeed involved, it is anticipated that SAK activity will be decreased in both cystic and non-cystic tubules of ADPKD kidneys where apoptosis is detected (Woo, 1995).

The present results also demonstrate the critical role of the F-actin/filamin A network in the regulation of SAKs by polycystins in kidney epithelial cells. We previously introduced the "Upholstery Model" to explain how polycystins may affect the conversion of intraluminal pressure to local bilayer tension (Sharif Naeini et al., 2009). We proposed that PC2 through interaction with filamin A and crosslinking of F-actin may influence the radius of membrane curvature in microdomains and thus, according to Laplace's Law, control membrane tension (Sharif Naeini et al., 2009). The PC2/filamin A interaction is predicted to occur whether PC2 is in the endoplasmic reticulum or at the plasma membrane because in both cases the C-terminal domain of PC2 will be facing the cytosol (Sharif Naeini et al., 2009). The deletion of the carboxy-terminal domain of PC2 at position 690, unlike at position 740, impairs the interaction with filamin A (our proteomic data; Sharif-Naeini et al., 2009), and moreover, PC2-690X fails to influence SACs (data not shown). In the present study we identify the molecular identity of the mechano-gated ion channels regulated by polycystins through the actin cytoskeletal network in renal tubular epithelial cells, with TREK-2 playing a key role in PCT cells. Because stimulation of SAKs by low pH_i or polyunsaturated fatty acids is not altered by polycystins, these modes of K_{2P} channel activation are likely to be independent of membrane tension or of the actin cytoskeletal network.

In conclusion we put forward a mechanism whereby a loss of mechanoprotection by SAKs (i.e., TREK/TRAAK K_{2P} channels)

enhances tubular cell death and contributes to kidney failure in ADPKD. Altogether, these results allow a better understanding of the molecular basis of renal mechanotransduction, mechano-protection, and involvement in disease states.

EXPERIMENTAL PROCEDURES

Electrophysiology

Electrophysiological procedure has been previously described elsewhere (Sharif Naeini et al., 2009). Briefly, single-channel cell-attached patch-clamp recordings were performed on primary cultures or immortalized PCT cells, as well as on transiently transfected COS-7, M2, or A7 cells. The pipette medium contained 150 mM NaCl, 5 mM KCl, 1 mM $CaCl_2$, and 10 mM HEPES (pH 7.4 with NaOH). The pipette solution also contained 10 mM TEA, 5 mM 4AP, and 10 μM glibenclamide to inhibit eventual contaminating potassium channels. The bath medium contained 155 mM KCl, 5 mM EGTA, 3 mM $MgCl_2$, and 10 mM HEPES (pH 7.2 with KOH). The osmolality of all solutions was adjusted to 310 mOsm. For HCO_3^- stimulation, 90 mM KCl was substituted with 90 mM $KHCO_3$. Membrane patches were stimulated with brief negative pressure pulses of -10 mm Hg increments, through the recording electrode using a pressure-clamp device (ALA High Speed Pressure Clamp-1 system; ALA Scientific). The holding voltage for all experiments was 0mV for SAK recordings. Detailed information is available in the Extended Experimental Procedures.

SUPPLEMENTAL INFORMATION

Supplemental Information includes Extended Experimental Procedures and seven figures and can be found with this article online at doi:10.1016/j.celrep.2012.01.006.

LICENSING INFORMATION

ACKNOWLEDGMENTS

REFERENCES

Bai, C.X., Kim, S., Li, W.P., Streets, A.J., Ong, A.C., and Tsiokas, L. (2008). Activation of TRPP2 through mDia1-dependent voltage gating. EMBO J. *27*, 1345–1356.

Bang, H., Kim, Y., and Kim, D. (2000). TREK-2, a new member of the mechanosensitive tandem-pore K+ channel family. J. Biol. Chem. *275*, 17412–17419.

Barriere, H., Belfodil, R., Rubera, I., Tauc, M., Lesage, F., Poujeol, C., Guy, N., Barhanin, J., and Poujeol, P. (2003). Role of TASK2 potassium channels regarding volume regulation in primary cultures of mouse proximal tubules. J. Gen. Physiol. *122*, 177–190.

Beck, J.S., and Potts, D.J. (1990). Cell swelling, co-transport activation and potassium conductance in isolated perfused rabbit kidney proximal tubules. J. Physiol. *425*, 369–378.

Blondeau, N., Pétrault, O., Manta, S., Giordanengo, V., Gounon, P., Bordet, R., Lazdunski, M., and Heurteaux, C. (2007). Polyunsaturated fatty acids are cerebral vasodilators via the TREK-1 potassium channel. Circ. Res. *101*, 176–184.

Boca, M., Distefano, G., Qian, F., Bhunia, A.K., Germino, G.G., and Boletta, A. (2006). Polycystin-1 induces resistance to apoptosis through the phosphatidylinositol 3-kinase/Akt signaling pathway. J. Am. Soc. Nephrol. *17*, 637–647.

Boletta, A., Qian, F., Onuchic, L.F., Bhunia, A.K., Phakdeekitcharoen, B., Hanaoka, K., Guggino, W., Monaco, L., and Germino, G.G. (2000). Polycystin-1, the gene product of PKD1, induces resistance to apoptosis and spontaneous tubulogenesis in MDCK cells. Mol. Cell *6*, 1267–1273.

Cemerikic, D., and Sackin, H. (1993). Substrate activation of mechanosensitive, whole cell currents in renal proximal tubule. Am. J. Physiol. *264*, F697–F714.

Chalfie, M. (2009). Neurosensory mechanotransduction. Nat. Rev. Mol. Cell Biol. *10*, 44–52.

Chen, X.Z., Segal, Y., Basora, N., Guo, L., Peng, J.B., Babakhanlou, H., Vassilev, P.M., Brown, E.M., Hediger, M.A., and Zhou, J. (2001). Transport function of the naturally occurring pathogenic polycystin-2 mutant, R742X. Biochem. Biophys. Res. Commun. *282*, 1251–1256.

Chevalier, R.L. (2008). Chronic partial ureteral obstruction and the developing kidney. Pediatr. Radiol. *38* (Suppl 1), S35–S40.

Delmas, P. (2004). Polycystins: from mechanosensation to gene regulation. Cell *118*, 145–148.

Derezic, D., and Cecuk, L. (1982). Hydrostatic pressure within renal cysts. Br. J. Urol. *54*, 93–94.

Edelstein, C.L. (2005). What is the role of tubular epithelial cell apoptosis in polycystic kidney disease (PKD)? Cell Cycle *4*, 1550–1554.

Garcia-Anoveros, J., and Corey, D.P. (1997). The molecules of mechanosensation. Annu. Rev. Neurosci. *20*, 567–594.

Garry, A., Fromy, B., Blondeau, N., Henrion, D., Brau, F., Gounon, P., Guy, N., Heurteaux, C., Lazdunski, M., and Saumet, J.L. (2007). Altered acetylcholine, bradykinin and cutaneous pressure-induced vasodilation in mice lacking the TREK1 potassium channel: the endothelial link. EMBO Rep. *8*, 354–359.

Goilav, B. (2011). Apoptosis in polycystic kidney disease. Biochim. Biophys. Acta *1812*, 1272–1280.

Grantham, J.J., Mulamalla, S., and Swenson-Fields, K.I. (2011). Why kidneys fail in autosomal dominant polycystic kidney disease. Nat. Rev. Nephrol. *7*, 556–566.

Guyon, A., Tardy, M.P., Rovère, C., Nahon, J.L., Barhanin, J., and Lesage, F. (2009). Glucose inhibition persists in hypothalamic neurons lacking tandem-pore K+ channels. J. Neurosci. *29*, 2528–2533.

Hahn, C., and Schwartz, M.A. (2009). Mechanotransduction in vascular physiology and atherogenesis. Nat. Rev. Mol. Cell Biol. *10*, 53–62.

Harris, P.C., and Torres, V.E. (2009). Polycystic kidney disease. Annu. Rev. Med. *60*, 321–337.

Honoré, E. (2007). The neuronal background K_{2P} channels: focus on TREK1. Nat. Rev. Neurosci. *8*, 251–261.

Honoré, E., Maingret, F., Lazdunski, M., and Patel, A.J. (2002). An intracellular proton sensor commands lipid- and mechano-gating of the K(+) channel TREK-1. EMBO J. *21*, 2968–2976.

Honoré, E., Patel, A.J., Chemin, J., Suchyna, T., and Sachs, F. (2006). Desensitization of mechano-gated K_{2P} channels. Proc. Natl. Acad. Sci. USA *103*, 6859–6864.

Jaalouk, D.E., and Lammerding, J. (2009). Mechanotransduction gone awry. Nat. Rev. Mol. Cell Biol. *10*, 63–73.

Kainulainen, T., Pender, A., D'Addario, M., Feng, Y., Lekic, P., and McCulloch, C.A. (2002). Cell death and mechanoprotection by filamin a in connective tissues after challenge by applied tensile forces. J. Biol. Chem. *277*, 21998–22009.

Kung, C. (2005). A possible unifying principle for mechanosensation. Nature *436*, 647–654.

Lantinga-van Leeuwen, I.S., Dauwerse, J.G., Baelde, H.J., Leonhard, W.N., van de Wal, A., Ward, C.J., Verbeek, S., Deruiter, M.C., Breuning, M.H., de Heer, E., and Peters, D.J. (2004). Lowering of Pkd1 expression is sufficient to cause polycystic kidney disease. Hum. Mol. Genet. *13*, 3069–3077.

Lauritzen, I., Zanzouri, M., Honoré, E., Duprat, F., Ehrengruber, M.U., Lazdunski, M., and Patel, A.J. (2003). K+-dependent cerebellar granule neuron apoptosis. Role of task leak K+ channels. J. Biol. Chem. *278*, 32068–32076.

Lauritzen, I., Chemin, J., Honoré, E., Jodar, M., Guy, N., Lazdunski, M., and Jane Patel, A. (2005). Cross-talk between the mechano-gated K_{2P} channel TREK-1 and the actin cytoskeleton. EMBO Rep. *6*, 642–648.

Lesage, F., Terrenoire, C., Romey, G., and Lazdunski, M. (2000). Human TREK2, a 2P domain mechano-sensitive K+ channel with multiple regulations by polyunsaturated fatty acids, lysophospholipids, and Gs, Gi, and Gq protein-coupled receptors. J. Biol. Chem. *275*, 28398–28405.

L'Hoste, S., Poet, M., Duranton, C., Belfodil, R., é Barriere, H., Rubera, I., Tauc, M., Poujeol, C., Barhanin, J., and Poujeol, P. (2007). Role of TASK2 in the control of apoptotic volume decrease in proximal kidney cells. J. Biol. Chem. *282*, 36692–36703.

Lumpkin, E.A., and Caterina, M.J. (2007). Mechanisms of sensory transduction in the skin. Nature *445*, 858–865.

Ma, R., Li, W.P., Rundle, D., Kong, J., Akbarali, H.I., and Tsiokas, L. (2005). PKD2 functions as an epidermal growth factor-activated plasma membrane channel. Mol. Cell. Biol. *25*, 8285–8298.

Maingret, F., Patel, A.J., Lesage, F., Lazdunski, M., and Honoré, E. (1999). Mechano- or acid stimulation, two interactive modes of activation of the TREK-1 potassium channel. J. Biol. Chem. *274*, 26691–26696.

Mulvany, M.J. (2002). Small artery remodeling and significance in the development of hypertension. News Physiol. Sci. *17*, 105–109.

Nauli, S.M., Alenghat, F.J., Luo, Y., Williams, E., Vassilev, P., Li, X., Elia, A.E., Lu, W., Brown, E.M., Quinn, S.J., et al. (2003). Polycystins 1 and 2 mediate mechanosensation in the primary cilium of kidney cells. Nat. Genet. *33*, 129–137.

Nauli, S.M., Kawanabe, Y., Kaminski, J.J., Pearce, W.J., Ingber, D.E., and Zhou, J. (2008). Endothelial cilia are fluid shear sensors that regulate calcium signaling and nitric oxide production through polycystin-1. Circulation *117*, 1161–1171.

Patel, A., and Honoré, E. (2010). Polycystins and renovascular mechanosensory transduction. Nat. Rev. Nephrol. *6*, 530–538.

Patel, A.J., and Lazdunski, M. (2004). The 2P-domain K+ channels: role in apoptosis and tumorigenesis. Pflugers Arch. *448*, 261–273.

Patel, A.J., Honoré, E., Maingret, F., Lesage, F., Fink, M., Duprat, F., and Lazdunski, M. (1998). A mammalian two pore domain mechano-gated S-like K+ channel. EMBO J. *17*, 4283–4290.

Pedersen, S.F., and Nilius, B. (2007). Transient receptor potential channels in mechanosensing and cell volume regulation. Methods Enzymol. *428*, 183–207.

Pei, Y. (2001). A "two-hit" model of cystogenesis in autosomal dominant polycystic kidney disease? Trends Mol. Med. *7*, 151–156.

Power, R.E., Doyle, B.T., Higgins, D., Brady, H.R., Fitzpatrick, J.M., and Watson, R.W. (2004). Mechanical deformation induced apoptosis in human proximal renal tubular epithelial cells is caspase dependent. J. Urol. *171*, 457–461.

Qian, F., Watnick, T.J., Onuchic, L.F., and Germino, G.G. (1996). The molecular basis of focal cyst formation in human autosomal dominant polycystic kidney disease type I. Cell *87*, 979–987.

Quinlan, M.R., Docherty, N.G., Watson, R.W., and Fitzpatrick, J.M. (2008). Exploring mechanisms involved in renal tubular sensing of mechanical stretch following ureteric obstruction. Am. J. Physiol. Renal Physiol. *295*, F1–F11.

Rohatgi, R., and Flores, D. (2010). Intratubular hydrodynamic forces influence tubulointerstitial fibrosis in the kidney. Curr. Opin. Nephrol. Hypertens. *19*, 65–71.

Sachs, F., and Morris, C.E. (1998). Mechanosensitive ion channels in nonspecialized cells. Rev. Physiol. Biochem. Pharmacol. *132*, 1–77.

Sackin, H. (1989). A stretch-activated K+ channel sensitive to cell volume. Proc. Natl. Acad. Sci. USA *86*, 1731–1735.

Sammels, E., Devogelaere, B., Mekahli, D., Bultynck, G., Missiaen, L., Parys, J.B., Cai, Y., Somlo, S., and De Smedt, H. (2010). Polycystin-2 activation by inositol 1,4,5-trisphosphate-induced Ca^{2+} release requires its direct association with the inositol 1,4,5-trisphosphate receptor in a signaling microdomain. J. Biol. Chem. *285*, 18794–18805.

Sandoz, G., Douguet, D., Chatelain, F., Lazdunski, M., and Lesage, F. (2009). Extracellular acidification exerts opposite actions on TREK1 and TREK2 potassium channels via a single conserved histidine residue. Proc. Natl. Acad. Sci. USA *106*, 14628–14633.

Sharif-Naeini, R., Folgering, J.H., Bichet, D., Duprat, F., Lauritzen, I., Arhatte, M., Jodar, M., Dedman, A., Chatelain, F.C., Schulte, U., et al. (2009). Polycystin-1 and -2 dosage regulates pressure sensing. Cell *139*, 587–596.

Tanner, G.A., Tielker, M.A., Connors, B.A., Phillips, C.L., Tanner, J.A., and Evan, A.P. (2002). Atubular glomeruli in a rat model of polycystic kidney disease. Kidney Int. *62*, 1947–1957.

Tao, Y., Kim, J., Faubel, S., Wu, J.C., Falk, S.A., Schrier, R.W., and Edelstein, C.L. (2005). Caspase inhibition reduces tubular apoptosis and proliferation and slows disease progression in polycystic kidney disease. Proc. Natl. Acad. Sci. USA *102*, 6954–6959.

Terrenoire, C., Lauritzen, I., Lesage, F., Romey, G., and Lazdunski, M. (2001). A TREK-1-like potassium channel in atrial cells inhibited by beta-adrenergic stimulation and activated by volatile anesthetics. Circ. Res. *89*, 336–342.

Tsiokas, L., Arnould, T., Zhu, C., Kim, E., Walz, G., and Sukhatme, V.P. (1999). Specific association of the gene product of PKD2 with the TRPC1 channel. Proc. Natl. Acad. Sci. USA *96*, 3934–3939.

Wei, F., Karihaloo, A., Yu, Z., Marlier, A., Seth, P., Shibazaki, S., Wang, T., Sukhatme, V.P., Somlo, S., and Cantley, L.G. (2008). Neutrophil gelatinase-associated lipocalin suppresses cyst growth by Pkd1 null cells in vitro and in vivo. Kidney Int. *74*, 1310–1318.

Wilson, P.D. (2004). Polycystic kidney disease. N. Engl. J. Med. *350*, 151–164.

Woo, D. (1995). Apoptosis and loss of renal tissue in polycystic kidney diseases. N. Engl. J. Med. *333*, 18–25.

Wozniak, M.A., and Chen, C.S. (2009). Mechanotransduction in development: a growing role for contractility. Nat. Rev. Mol. Cell Biol. *10*, 34–43.

Wu, G., D'Agati, V., Cai, Y., Markowitz, G., Park, J.H., Reynolds, D.M., Maeda, Y., Le, T.C., Hou, H., Jr., Kucherlapati, R., et al. (1998). Somatic inactivation of Pkd2 results in polycystic kidney disease. Cell *93*, 177–188.

Wyker, A.T., Ritter, R.C., Marion, D., and Gillenwater, J.Y. (1981). Mechanical factors and tissue stresses in chronic hydronephrosis. Invest. Urol. *18*, 430–436.

Zhou, J. (2009). Polycystins and primary cilia: primers for cell cycle progression. Annu. Rev. Physiol. *71*, 83–113.

Supplemental Information

EXTENDED EXPERIMENTAL PROCEDURES

Cell Culture and Transfection

Culture of COS, A7, and M2 Cells. COS-7 cell lines were cultured in Dulbecco's Modified Eagle's Medium (GIBCO BRL Life Technologies) supplemented with 10% fetal calf serum (Hyclone). A7 and M2 cells (a gift from Dr. T.P. Stossel) were cultured as previously described (Sharif Naeini et al., 2009).

Isolation and Culture of Mouse Primary PCT Cells. 5-6 weeks old C57Bl/6 females and mutants mice were used. Proximal convoluted tubules were microdissected under sterile conditions. Kidneys were perfused with Hanks' solution (GIBCO) containing 700 kU/l collagenase (Worthington), cut into small pyramids that were incubated for 1 hr at room temperature in the perfusion buffer (160 kU/l collagenase, 1% Nuserum, and 1 mM $CaCl_2$), and continuously aerated. The pyramids were then rinsed thoroughly in the same buffer devoid of collagenase. The individual nephrons were dissected by hand in this buffer under binoculars using stainless steel needles mounted on Pasteur pipettes. PCT corresponded to the 1 to 1.5 mm segment of tissue located immediately after the glomerulus. After they were rinsed in the dissecting medium, tubules were transferred to collagen-coated 35-mm Petri dishes filled with culture medium composed of equal quantities of DMEM and Ham's F-12 (GIBCO) containing 15 mM $NaHCO_3$, 20 mM HEPES, pH 7.4, 1% serum, 2 mM glutamine, 5 mg/l insulin, 50 nM dexamethasone, 10 μg/l epidermal growth factor, 5 mg/l transferrin, 30 nM sodium selenite, and 10 nM triiodo-L-thyronine. Cultures were maintained at 37°C in a 5% CO_2-95% air water-saturated atmosphere. The medium was removed 4 days after seeding and then every 2 days. QPCR experiments indicated that both *Pkd1* and *Pkd2* are expressed in WT PCT cells (Figure S7).

Immortalization of WT, TREK-2$^{-/-}$, and TREK-1/TREK-2/TRAAK$^{-/-}$ Mouse PCT Cells. 10-day-old primary cultures of mouse proximal tubules were transfected with pSV3 *neo* using Lipofectin (Invitrogen). After 48 hr, selection of the clones was performed by the addition of G418 (500 μg/ml). Culture medium (Dulbecco's modified Eagle's medium-F12, Sigma, Saint Quentin Fallavier, France) containing 125 μg/ml G418, 15 mM $NaHCO_3$, 20 mM HEPES (pH 7.4), growth factors, and 1% Fetal Calf Serum was changed every day. Resistant clones were isolated, subcultured, and used after 10 trypsinization steps. Immortalized proximal wild-type (WT), TREK-2$^{-/-}$ and TREK-1$^{-/-}$/TREK-2$^{-/-}$/TRAAK$^{-/-}$ (SAKs) KO cell lines were grown on collagen-coated supports (35-mm Petri dishes) in a 5% CO_2 atmosphere at 37°C in the culture medium described above.

Isolation of Pkd1$^{-/-}$ Cells. Proximal tubule cell lines null (PN24) and heterozygous (PH2) for *Pkd1* were made from a single mouse carrying a conditional allele for *Pkd1* and the conditionally immortalizing ImmortoMouse (H-2Kb-tsA58) transgene as previously described (Wei et al., 2008). Briefly, the null and heterozygous cell lines were clonally derived from single parental *Pkd1$^{lox/-}$* clones following transient transfection with Cre recombinase.

Culture and Differentiation of Pkd1$^{lox/-}$ and Pkd1$^{-/-}$ Cells. PCT cells were maintained and passaged in DMEM/F12 supplemented with: 3% FCS, γ interferon 5 μg/ml, sodium selenite 7.5 nM, Triiodo-L-Thyronine 1.9 nM, insulin 5 mg/l, transferrin 5 mg/l, penicillin-streptomycin 100 u/ml, nystatin 5 ml/l (all products from Sigma-Aldrich) at 33°C with 5% CO_2. Cells were changed to γ-interferon-free, 1% Fetal Calf Serum medium 7 days before usage in the described experiments and maintained at 37°C to suppress large T antigen expression. Q PCR experiments confirmed the absence of *Pkd1* in the *Pkd1$^{-/-}$* cells (Figure S7).

Transfection. COS-7 cells were transfected using a modified DEAE-Dextran protocol as previously described (Fink et al., 1996). PCT cells were transfected using jetPEI (polyplus transfection) according to the manufacturer's instructions and 2 μg of plasmid DNA were used per dish. A7 and M2 cells were transfected as previously described (Sharif Naeini et al., 2009). TRPC1 or the disease-causing mutant PC2 740X (inserted into pIRES$_2$-EGFP or DsRed vectors) were transfected at 0.5 μg of plasmid DNA per 35mm dish containing ~25 000 cells per dish. TREK-1 and TREK-2 were transfected at 0.03 μg and TRAAK was transfected at 0.01 μg (cloned into a pIRES$_2$-EGFP vector). Human TASK2 cloned in a pIRES$_2$-CD8 vector was transfected at 0.1 μg.

Molecular Biology

The mPC2 (Entrez GeneID: 5311) deletion construct, corresponding to the human pathogenic R742X mutant (mPC2-740X) (Qian et al., 1997), was generated by PCR and cloned into either a pIRES$_2$-EGFP or a pIRES$_2$-DsRed vector. All inserts were sequenced in their entirety.

QPCR experiments were performed using Sybr green on a Light Cycler 480 (Roche). QPCR expression of *Pkd1* and *Pkd2* in mouse renal isolated tubules and in the various PCT cell lines is illustrated in Figure S7. siRNAs directed against *Pkd2* as well as transfection method have been previously described (Sharif Naeini et al., 2009). Oligonucleotide sequences are available upon request.

Biotinylation Experiments. COS cells were seeded at 1.3 million cells per 60 mm plate the day before transfection. Cells were transfected with 5 μg of each plasmid: 1. HA-TREK 1 + empty vector; 2. HA-TREK-1+ MYC-PC2 740X; 3. HA-TREK 1 + MYC-PC2. The biotinylation experiment was carried out 48 hr post transfection. Cells were rinsed 3 times with PBS+ (0.1mM $CaCl_2$, 1mM $MgCl_2$ in PBS-). Each plate was incubated with 2 ml of PBS+ with 0.5 mg/ml of Sulfo NHS LC biotin Pierce for 30 min at 4°C. Cells were then rinsed 3 times with PBS-. Cells were then scraped into 500 μl of lysis buffer containing: 10 mM Tris Cl pH 7.4, 150 mM NaCl, 1mM EDTA, 1mM EGTA, 1% Triton X-100, 0.5% NP40 supplemented with protease inhibitors. Lysate was sonicated and incubated at 4°C for 30 min. Lysates were then centrifuged at 4°C for 5 min at 14K rpm. 30 μl of the supernatant was taken for input. The rest of the supernatant received 25 μl of Streptavidin magnetic particles (Roche). Samples were rotated in the cold room for 1hr. Biotin labeled molecules then pulled down using a magnetic particle concentrator. The beads were washed 3 times with lysis buffer and

resuspended in gel loading buffer for analysis. Gels were charged with the input samples and biotinylation samples. Each blot was cut between the 75 and 50 KDa marker to allow detection of either HA (under 75 KDa) or MYC (at or above 75 KDa) on the same blot. Lower blots were stripped and reprobed with anti-actin.

Animals

All experiments were performed according to policies on the care and use of laboratory animals of European Community Legislation. All efforts were made to minimize animal suffering and reduce the number of animals used. The animals housed under controlled laboratory conditions with a 12-h dark–light cycle, a temperature of $21 \pm 2°C$, and a humidity of 60%–70% had free access to standard rodent diet and tap water. TREK-2 and SAK KO mice have been previously described in (Guyon et al., 2009). $Pkd1^{+/-}$ mice were described in (Lantinga-van Leeuwen et al., 2007). The genetic background of these mice was C57Bl6.

Surgical Procedure

10-day-old male mice were subjected to complete left unilateral ureteral obstruction or sham-operation. Under general anesthesia with isoflurane and oxygen, the abdomen was surgically opened by a left lateral incision; the left ureter was exposed and a 8-0 ethilon suture was placed (the ureter was not transected), or were left unligated (sham). The incision was closed by suturing. For postoperative analgesia, the animals were injected IP once with 0.01mg/kg buprenorphine (Sigma). The animals were allowed to recover from anesthesia and returned to their mothers.

Normal pressure within the renal pelvis and ureter is about 0-7 mm Hg. Following acute ureteral obstruction, there is an abrupt rise in pressure which may exceed 60 mm Hg (Power et al., 2004; Quinlan et al., 2008; Wyker et al., 1981). Subsequently, pelvic pressure will drop over time (within weeks) because of dilation of the renal pelvis, decrease in both blood flow and glomerular filtration rate and altered pyelolymphatic and pyelovenous backflow (Wyker et al., 1981). However, according to the law of Laplace, renal wall stress will continue to build up with time (even though pressure drops) because of the increase in renal volume (higher radius of curvature) and wall thinning (Wyker et al., 1981).

After 3 days of obstruction, animals were sacrificed, and their kidneys were removed, measured and weighed.

Histology

The organs were dissected, decapsulated and fixed in 4% paraformaldehyde in DPBS (Dulbecco's Phosphate Buffered Saline; GIBCO BRL Life Technologies) for 48 hr. Fixed tissues were dehydrated in graded ethanol and xylene and embedded in paraffin. Sequential sections of 7 μm were mounted onto Superfrost-plus glass slides. After deparaffinization, sections were stained with hematoxylin and eosin. Tubular area was measured using the Image J software.

Identification of Cellular Apoptosis: *In Vitro Assays.* Cells were grown in 35 mm culture fluorodish (WPI) coated with collagen and containing 3 ml of culture medium (20 000 cells per plate). 3 days after seeding, apoptosis was induced by mechanical stress associated with centrifugation of the plates for 4 hr at 2800 × g (37°C, HEPES buffer) and analyzed after a recovery period of 3 hr in the incubator (HCO_3^- buffer). Early stage apoptosis was quantified using Annexin-V-Fluos (Roche, Mannheim, Germany), 15 min at room temperature in the dark with Annexin V (1/100). Late stage cell death was quantified using a Hoechst 33342 staining at 50 μg/ml for 10 min at room temperature (Molecular Probe, H3570). Nuclear morphology was displayed on a Zeiss Axio Observer fluorescence microscope (405-435 nm). Mean of 400 images analyzed per condition, each containing ∼40 cells. When studying the effect of PC2-740X expression, PCT transfected cells were visualized by EGFP fluorescence (IRES EGFP plasmid) and only the Hoechst staining was performed and quantified.

Activation of SACs in patch clamp experiments requires tension on the order of 1-5 mN/m (Sachs and Morris, 1998). Can centrifugation produce such stress in the membrane? The effect of the surrounding solution is to simply raise the hydrostatic pressure, but since the cell is also composed mostly of water, hydrostatic compression effects will be minimal. The most likely transduction is via changes in cell shape induced by the higher density of the cell interior (specific gravity ∼1.05). To calculate these forces would require finite element numerical analyses utilizing the density of the cell components, as well as elasticity and estimates of water movement under pressure, but that data is not available currently. Alternatively, as a simplified model, consider a spherical cell (radius R_0 = 10 μm) resting on a rigid substrate. Take the simplest case of the cell squished down to a hemisphere by centrifugation. The cell volume is $V_0 = 4/3\pi R_0^3$. If we assume that no water leaves the cell, the ending volume of the hemisphere is the same as the starting volume of the sphere $V_c = 2/3\pi R_c^3$. Solving, $R_c = \sqrt[3]{2}R_0$. The increase in radius will stretch the cell membrane. Before centrifugation the cell area is $A_0 = 4\pi R_0^2$ and the area after centrifugation is that of a hemisphere $A_c = 2\pi R_c^2 = 1.6R_0^2$ plus the area where the cell contacts the substrate, $A_d = \pi R_c^2$. The fractional change in area $\Delta A/A = (A_c-A_0)/A_0 = 0.19$. The membrane tension is $T = k_a\Delta A/A = 0.19k_a$ where k_a is the elastic constant of the membrane. Since k_a is commonly in the range of 100 mN/m for biological membranes (Rawicz et al., 2008), the membrane tension is estimated to be about 20 mN/m. Thus, this simplified model suggests that membrane tension from centrifugation may be sufficient to change the gating of SACs.

In Situ Assays. Terminal deoxynucleotidyl transferase (TdT)-mediated 2′-deoxyuridine 5′-triphosphate-biotin nick-end labeling (TUNEL) staining was performed by using the In Situ Cell Death Detection Kit (Roche, Mannheim, Germany). Labeling of 3′-OH terminal DNA fragments was then performed at room temperature for 1 hr by using the TUNEL reaction mixture according to the manufacturer's protocol. Red labeling was used to avoid the high green autofluorescence of kidney. In addition, sections were double stained with Hoechst 33342 (Molecular Probe, H3570, at 50 μg/ml for 10 min at room temperature) to visualize all the nuclei

in the field and identify fragmented nuclei. For both staining, percentage of cell death was determined in the same region by counting 18 random fields (mean of 250 cells) per kidney. The sections were observed under a Zeiss Axio Observer fluorescence microscope.

Statistical Analysis

Significance was tested with a permutation test (R Development Core Team: http://www.r-project.org/) (n < 30) or two samples t Test (n > 30). One star indicates p < 0.05, two stars p < 0.01 and three stars p < 0.001. Data represent mean ± standard error of the mean.

Standard error on the ratio $M_t/M_{mock} = S_t/M_{mock}$ with M_t: mean of treated population, M_{mock}: mean of mock population, S_t: standard error of treated population.

SUPPLEMENTAL REFERENCES

Fink, M., Duprat, F., Lesage, F., Reyes, R., Romey, G., Heurteaux, C., and Lazdunski, M. (1996). Cloning, functional expression and brain localization of a novel unconventional outward rectifier K^+ channel. EMBO J. *15*, 6854–6862.

Guyon, A., Tardy, M.P., Rovère, C., Nahon, J.L., Barhanin, J., and Lesage, F. (2009). Glucose inhibition persists in hypothalamic neurons lacking tandem-pore K^+ channels. J. Neurosci. *29*, 2528–2533.

Lantinga-van Leeuwen, I.S., Leonhard, W.N., van der Wal, A., Breuning, M.H., de Heer, E., and Peters, D.J. (2007). Kidney-specific inactivation of the Pkd1 gene induces rapid cyst formation in developing kidneys and a slow onset of disease in adult mice. Hum. Mol. Genet. *16*, 3188–3196.

Power, R.E., Doyle, B.T., Higgins, D., Brady, H.R., Fitzpatrick, J.M., and Watson, R.W. (2004). Mechanical deformation induced apoptosis in human proximal renal tubular epithelial cells is caspase dependent. J. Urol. *171*, 457–461.

Qian, F., Germino, F.J., Cai, Y., Zhang, X., Somlo, S., and Germino, G.G. (1997). PKD1 interacts with PKD2 through a probable coiled-coil domain. Nat. Genet. *16*, 179–183.

Quinlan, M.R., Docherty, N.G., Watson, R.W., and Fitzpatrick, J.M. (2008). Exploring mechanisms involved in renal tubular sensing of mechanical stretch following ureteric obstruction. Am. J. Physiol. Renal Physiol. *295*, F1–F11.

Rawicz, W., Smith, B.A., McIntosh, T.J., Simon, S.A., and Evans, E. (2008). Elasticity, strength, and water permeability of bilayers that contain raft microdomain-forming lipids. Biophys. J. *94*, 4725–4736.

Sachs, F., and Morris, C.E. (1998). Mechanosensitive ion channels in nonspecialized cells. Rev. Physiol. Biochem. Pharmacol. *132*, 1–77.

Sharif-Naeini, R., Folgering, J.H., Bichet, D., Duprat, F., Lauritzen, I., Arhatte, M., Jodar, M., Dedman, A., Chatelain, F.C., Schulte, U., et al. (2009). Polycystin-1 and -2 dosage regulates pressure sensing. Cell *139*, 587–596.

Wei, F., Karihaloo, A., Yu, Z., Marlier, A., Seth, P., Shibazaki, S., Wang, T., Sukhatme, V.P., Somlo, S., and Cantley, L.G. (2008). Neutrophil gelatinase-associated lipocalin suppresses cyst growth by Pkd1 null cells in vitro and in vivo. Kidney Int. *74*, 1310–1318.

Wyker, A.T., Ritter, R.C., Marion, D., and Gillenwater, J.Y. (1981). Mechanical factors and tissue stresses in chronic hydronephrosis. Invest. Urol. *18*, 430–436.
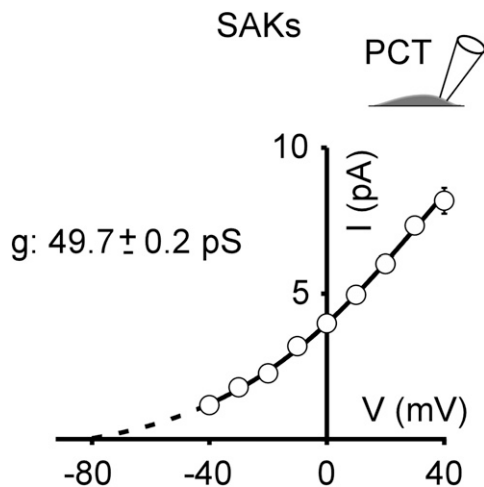
Figure S1. Native SAKs in PCT Cells, Related to Figure 2

i-V curve of the native SAKs in PCT cells recorded in the cell attached patch configuration in a physiological K$^+$ gradient (n = 5). The i-V curve was fitted with a Goldman-Hodgkin-Katz relationship and extrapolated in the negative voltage range. The extrapolated reversal potential is about -80 mV. The single channel conductance 49.7 $\pm$ 0.2 pS was estimated by linear regression in the range of -10 to 40 mV. Data represent mean $\pm$ standard error of the mean.
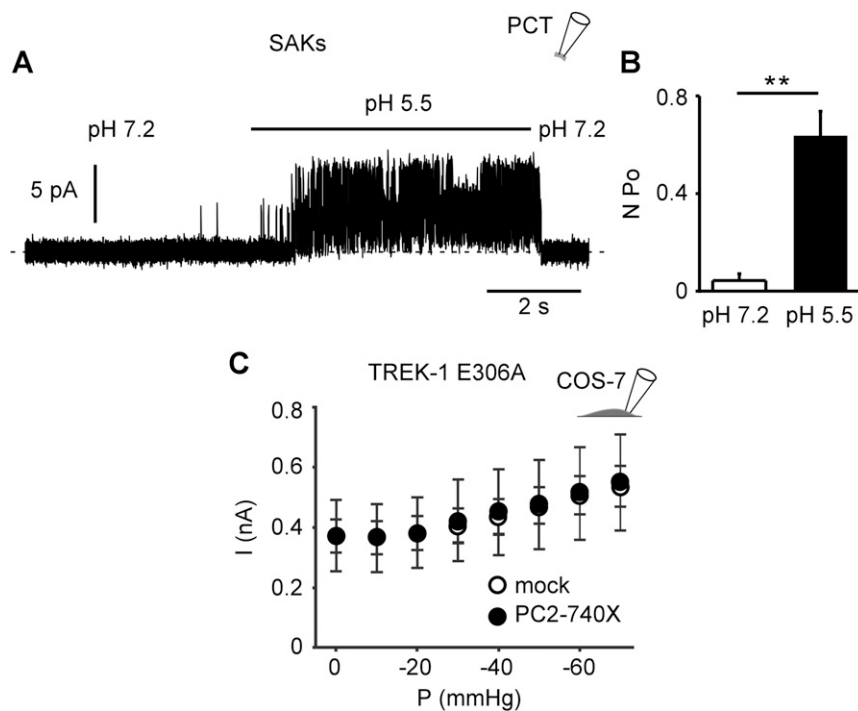
Figure S2. Activation of Native SAKs in PCT Cells by Intracellular Acidosis, Related to Figure 4

(A) Lowering intracellular pH from 7.2 to 5.5 induces the opening of native SAKs in PCT cells recorded at a holding potential of 0 mV in the inside out configuration.

(B) SAKs stimulation by intracellular acidosis to pHi 5.5 (black bar; n = 5) as compared to pHi 7.2 (white bar; n = 5).

(C) The mutant TREK-1 E306A transfected in COS cells and recorded at a holding potential of 0 mV in the cell attached patch configuration is locked open and shows no significant sensitivity to membrane stretch. E306A activity is not affected by PC2-740X expression (filled dots; n = 20) in comparison with a mock condition (empty dots; n = 19). Data represent mean ± standard error of the mean.
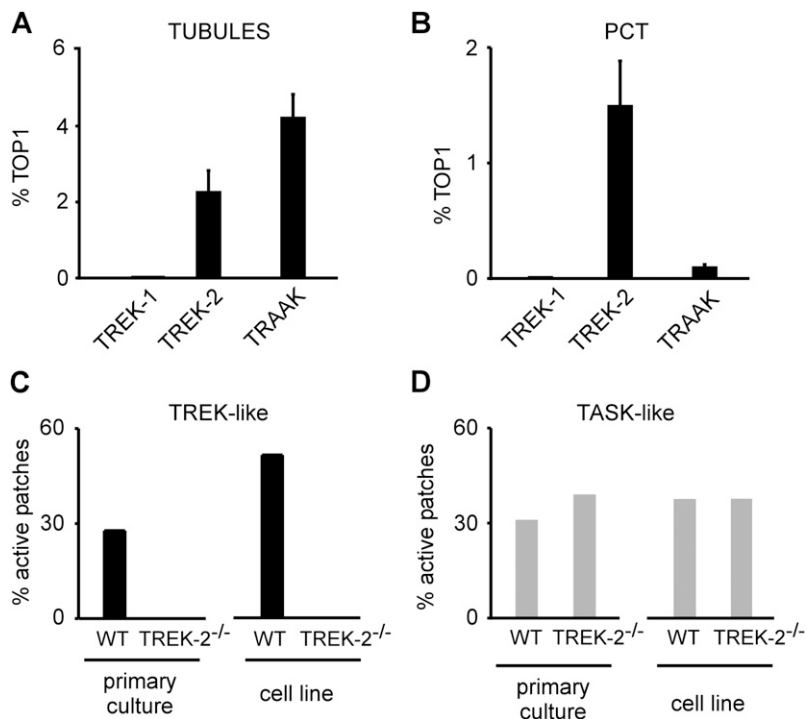
Figure S3. Expression of the TREK/TRAAK Subunits in PCT Cells, Related to Figures 2, 4, 5, and 6

(A) Relative expression to TOP1 of TREK-1 (n = 6), TREK-2 (n = 6) and TRAAK (n = 6) in mouse isolated whole renal tubules (proximal + distal).

(B) Same as (A) in cultured immortalized PCT cells (n = 7 for TREK-1, TREK-2 and TRAAK).

(C) SAKs recorded in the inside-out configuration at a holding potential of 0 mV are absent in PCT cells isolated from TREK-2 $^{-/-}$ mice (n = 70), as compared to WT cells (n = 36). Cells were either maintained in primary culture or grown after immortalization (n = 72 for WT and n = 43 for TREK-2 $^{-/-}$) as indicated.

(D) Lack of effect of TREK-2 inactivation on the TASK-like channel activity in PCT cells recorded in the cell-attached configuration at 0 mV in primary culture (n = 36 and n = 70 for WT and TREK-2 $^{-/-}$, respectively) or immortalized cell line (n = 72 and n = 43 for WT and TREK-2 $^{-/-}$, respectively). Data represent mean ± standard error of the mean.
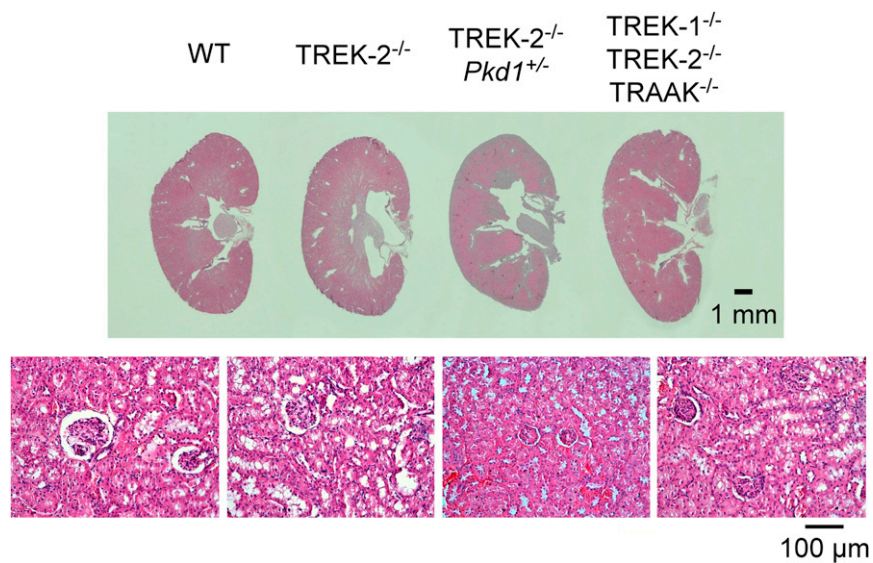
Figure S4. TREK/TRAAK Genetic Inactivation and Kidney Structure, Related to Figure 6

Sections of adult kidneys (from 33 to 75 weeks old) stained with eosin hematoxylin from WT (n = 3), TREK-2$^{-/-}$ (n = 4), TREK-2$^{-/-}$/Pkd1$^{+/-}$ (n = 6) and TREK-1/TREK-2/TRAAK (SAKs KO) mice (n = 2). Lower panels show sections in the cortical region for each kidney at higher magnification.
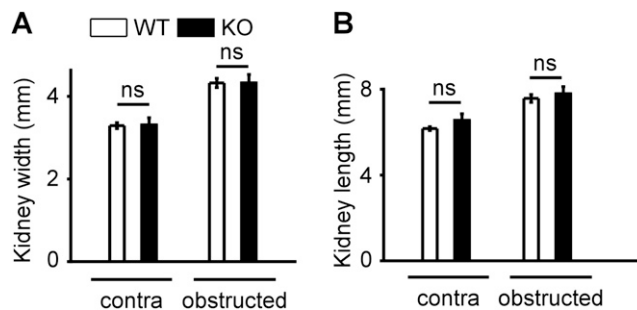
Figure S5. Morphology of Kidneys with Unilateral Ureteral Ligation from WT and SAK KO Mice, Related to Figure 6

(A) Ureteral ligation (obstructed) for 3 days in 10-day-old mice induces a significant increase in kidney width, as compared to the contralateral unligated kidney (n = 12 for WT shown with white bars and n = 12 for SAK KO shown with black bars).

(B) Ureteral ligation for 3 days in 10-day-old mice induces an increase in kidney length, as compared to the contralateral unligated kidney (n = 12 for WT shown with white bars and n = 12 for SAK KO shown with black bars). Data represent mean ± standard error of the mean.
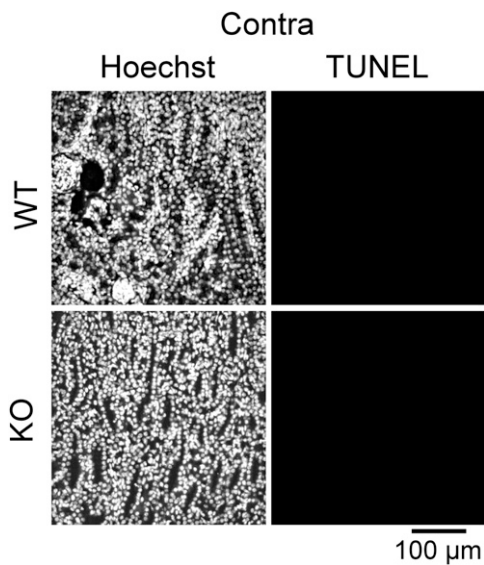
Figure S6. Absence of Apoptosis in WT and SAK KO Contralateral Kidneys, Related to Figure 6

No apoptotic cell detected by a double Hoechst (left panels) and TUNEL staining (right panels) on sections of WT mouse kidney contralateral (left panels; n = 14) or SAK KO (right panels; n = 13).
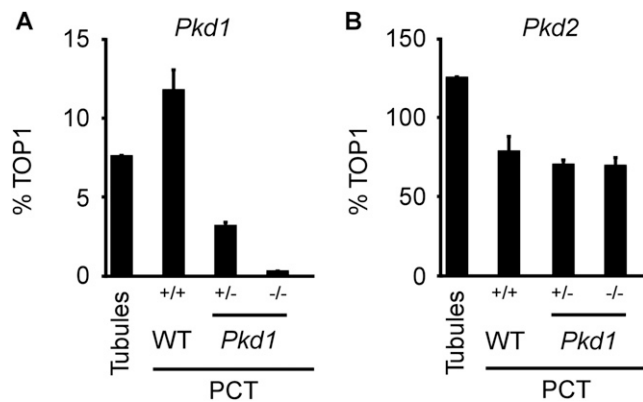
Figure S7. Pkd1 and Pkd2 Expression in Isolated Mouse Renal Tubules and in Cultured Immortalized PCT Cells, Related to Figures 1, 2, 4, and 5

(A) Expression of *Pkd1* (normalized to TOP1) in mouse renal isolated whole tubules (proximal + distal), as well as in the various PCT cell lines used in the present study, as determined by real-time QPCR.

(B) Expression of *Pkd2* in mouse renal isolated whole tubules (proximal + distal), as well as in the various PCT cell lines used in the present study, as determined by real-time QPCR. Data represent mean ± standard error of the mean. n values range from 3 to 7.